Science

Direct Observations of Interstellar H, He, and O by the Interstellar Boundary Explorer

E. Möbius, *et al.*

Science **326**, 969 (2009);
DOI: 10.1126/science.1180971

Direct Observations of Interstellar H, He, and O by the Interstellar Boundary Explorer

E. Möbius,[1]* P. Bochsler,[1,2] M. Bzowski,[3] G. B. Crew,[4] H. O. Funsten,[5] S. A. Fuselier,[6] A. Ghielmetti,[6] D. Heirtzler,[1] V. V. Izmodenov,[7,8] M. Kubiak,[3] H. Kucharek,[1] M. A. Lee,[1] T. Leonard,[1] D. J. McComas,[9,10] L. Petersen,[1] L. Saul,[2] J. A. Scheer,[2] N. Schwadron,[11] M. Witte,[12] P. Wurz[2]

Neutral gas of the local interstellar medium flows through the inner solar system while being deflected by solar gravity and depleted by ionization. The dominating feature in the energetic neutral atom Interstellar Boundary Explorer (IBEX) all-sky maps at low energies is the hydrogen, helium, and oxygen interstellar gas flow. The He and O flow peaked around 8 February 2009 in accordance with gravitational deflection, whereas H dominated after 26 March 2009, consistent with approximate balance of gravitational attraction by solar radiation pressure. The flow distributions arrive from a few degrees above the ecliptic plane and show the same temperature for He and O. An asymmetric O distribution in ecliptic latitude points to a secondary component from the outer heliosheath.

Interstellar neutral gas flows through the inner heliosphere due to the Sun's motion relative to the local interstellar medium (LISM), thus making interstellar gas measurements possible from Earth's orbit. Ionization of neutral atoms approaching the Sun and the Sun's gravitational field result in a characteristic flow pattern and density structure in the inner heliosphere with a cavity close to the Sun and gravitational focusing on the downwind side (Fig. 1A). For H this pattern is distinctly modified by radiation pressure, eliminating the downwind focusing. Previous LISM H and He diagnostic studies used ultraviolet backscatter observations (*1*, *2*), pickup ion studies (*3*, *4*), and a combination of methods for He (*5*). Making use of the Sun's gravitational deflection, the velocity distributions of various species can be studied in detail using neutral atom imagers (*6*, *7*) to derive interstellar gas parameters, filtering of the species in the outer heliosheath, and their deflection by interstellar magnetic field effects on the plasma. Previously, only neutral He had been observed, first by Ulysses outside 1.5 astronomical units (AU) (*8*, *9*) and then by IMAGE at 1 AU (*10*). Here, we present Interstellar Boundary Explorer (IBEX) observations of the interstellar neutral H, He, and O flow from January through April 2009. With the IBEX sensors pointing radially outward on a spacecraft whose spin axis points Sunward (*11*), the LISM flow is in the IBEX-Lo sensor field of view (FOV) in the spring, when Earth (and IBEX) move into the flow, and in the fall, when Earth recedes from the flow (*7*) (Fig. 1A).

The LISM flow dominates the IBEX-Lo all-sky maps at 15 and 110 eV with rates that exceed those of the diffuse energetic neutral atom (ENA) distributions (*12*–*14*) by up to four orders of magnitude (Fig. 1, B and C). The intense flow started with orbit 9 (mid-December 2008), peaked in orbit 16 (about –135° ecliptic longitude), and was seen through orbit 26 (April 2009) at 15 eV (Fig. 1B), but only through orbit 22 at 110 eV (Fig. 1C). A much narrower peak, maximized in orbit 16, showed up in the O maps for 280 eV and 600 eV (600 eV shown in Fig. 1D), with a tail extending from this peak toward higher latitude (up to about 20°) and smaller longitude (about –165°). The peak flux in all three maps arrives from slightly above the ecliptic plane. Based on the expected interstellar bulk flow energies at 1 AU for an observer that moves into flow with Earth's velocity, the distribution observed at 280 and 600 eV is largely interstellar O (529 eV bulk flow energy in the observer frame), the distribution seen up to 110 eV stems from interstellar He (132 eV), and the extended distribution seen into April at 15 eV is interstellar H (16 eV if radiation pressure cancels gravitational attraction).

With its time-of-flight (TOF) mass spectrometer, IBEX-Lo directly determines incoming neutral gas species after their conversion into negative ions on a diamond-like carbon conversion surface for H and O (*15*). However, He only produces a few metastable negative ions at higher energies (*16*). Therefore, it is identified in the TOF system through a well-characterized mixture of H, C, and

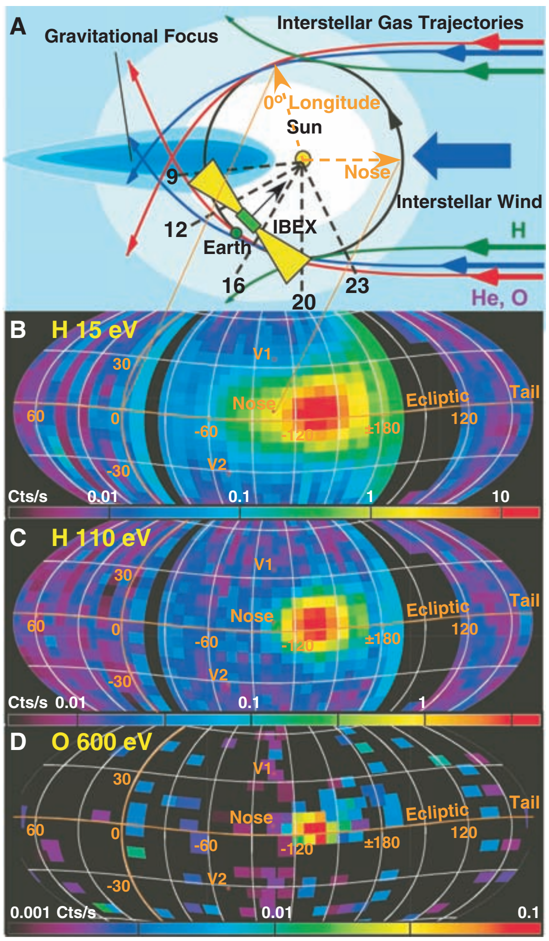

Fig. 1. (**A**) Schematic diagram of the interstellar gas flow through the inner heliosphere as deflected by the Sun's gravitational field. He and O trajectories are bent toward the Sun, stronger for slower atoms (red) than for faster ones (blue), making the bulk of them tangential to Earth's orbit for IBEX orbit 16, whereas H trajectories (green) are diverted outward by the Sun's radiation pressure. The color shading indicates the density pattern of He with its focusing cone. Also shown are Earth's positions for IBEX orbits 9 to 23 and the IBEX FOV for orbit 14. (**B**) H all-sky map (viewing direction) at 15 eV in a Mollweide projection (*12*) with color-coding of the count rate on a logarithmic scale after culling times with background from the magnetosphere and upstream particles (*12*). Black pixels either have zero counts or are culled for foreground from the magnetosphere (in particular in orbits 27 to 30, looking backward relative to Earth's motion, and all around in orbit 31). An intense flow is seen from –180° (orbit 9) to –50° (orbit 26) ecliptic longitude, that is, looking forward, with wide spread in latitude, and well away from potential magnetospheric interference. (**C**) H map at 110 eV with intense flow from –180° to –100° ecliptic longitude. (**D**) O map at 600 eV with intense flow from –165° to –110° ecliptic longitude.

[1]Space Science Center and Department of Physics, University of New Hampshire, Durham, NH 03824, USA. [2]Physikalisches Institut, Universität Bern, 3012 Bern, Switzerland. [3]Space Research Centre, Polish Academy of Sciences, 00-716 Warsaw, Poland. [4]Massachusetts Institute of Technology, Cambridge, MA 02139, USA. [5]Los Alamos National Laboratory, Los Alamos, NM 87545, USA. [6]Lockheed Martin Advanced Technology Lab, Palo Alto, CA, USA. [7]Moscow State University, 119899 Moscow, Russia. [8]Space Research Institute, Russian Academy of Sciences, 117997 Moscow, Russia. [9]Southwest Research Institute, San Antonio, TX 78228, USA. [10]University of Texas at San Antonio, San Antonio, TX 78249, USA. [11]Department of Astronomy, Boston University, Boston, MA 02215, USA. [12]Max-Planck-Institute for Solar System Research, 37191 Katlenburg-Lindau, Germany.

*To whom correspondence should be addressed. E-mail: Eberhard.moebius@unh.edu

Table 1. Observed species branching ratios. Shown in the first two rows are the C+O percentages of the total number of counts observed in the TOF spectra at 15, 29, 55, and 110 eV, after subtracting underlying H from diffuse ENAs (*12–14*), and in the third row (in italics) the C+O percentage found during calibration with a He beam at 110 eV and close to the actual LISM energy at 135 eV. The fourth row shows the observed C+O percentages for H at 15 eV and for O at 600 eV; the corresponding values from calibration are shown in the last row (in italics).

	E(eV)	%C+O	E(eV)	%C+O	E(eV)	%C+O	E(eV)	%C+O
Orbits 10 & 11	15	7	29	6	55	8	110	14
Orbits 13–19	15	14	29	18	55	16	110	11
110 & 135 eV He	*15*	*11 & 14*	*29*	*13 & 20*	*55*	*11 & 19*	*110*	*8 & 13*
Orbit 23	15	1			Orbits 16–18		600	100
15 & 29 eV H	*15*	*0–1*			*600 eV O*		*600*	*99*

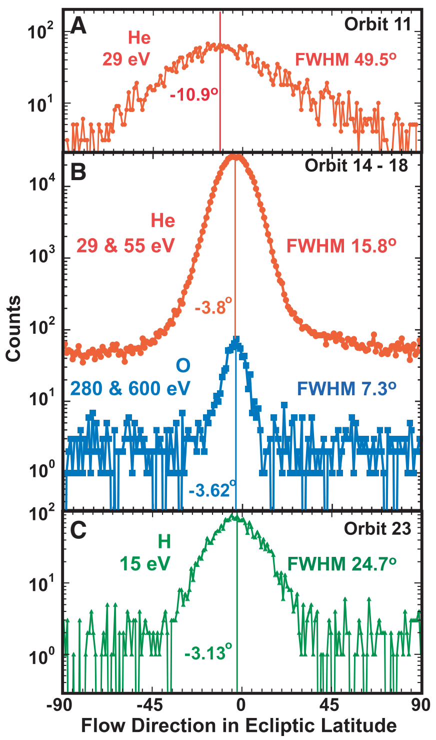

Fig. 2. Observed flow distributions as counts per 1° bin in ecliptic latitude for He [red, orbits 11 (**A**) and 14 to 18 (**B**)], O [blue, orbits 14 to 18 (B)], and H [green, orbit 23 (**C**)]. LISM H was seen only at 15 eV, sputter products of He at 15 to 110 eV (29 to 55 eV shown here), and O at 280 to 600 eV. The center position and FWHM of each distribution is shown, obtained with a Gaussian fit for the incoming flow convoluted with the IBEX-Lo angular response function.

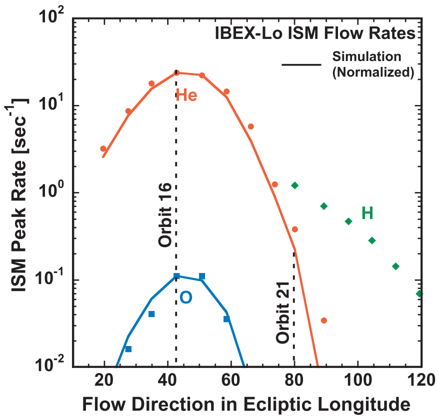

Fig. 3. Orbit-averaged count rates at the peak of the angular distributions (compare Fig. 2) for He, O, and H as a function of observed flow direction (after gravitational deflection at 1 AU) for orbits 13 (IBEX spin axis orientation finalized) through 26, together with the simulated rate for He and O, normalized to the observed rates at the maximum in orbit 16. These observed rates correspond to peak fluxes of 4.6×10^5 s^{-1} cm^{-2} sr^{-1} for He and 1.3×10^3 s^{-1} cm^{-2} sr^{-1} for O, based on the IBEX-Lo calibration. The LISM flow simulations use a hot interstellar gas model (*21*) with a flow speed of 26.3 km s^{-1} and temperature of 6300 K (*9*) for both He and O. The simulated distributions were accumulated for each orbit over the IBEX-Lo FOV in the actual spin axis orientation. The H rates in orbits 21 and 22 may contain small contaminations (25% and 4%) from He sputter products.

O that are sputtered from the conversion surface at energies below that of the incoming He.

For orbits 13 to 19, the observed composition reflected that from calibration (Table 1). At slightly lower energy, He produced substantially less C+O. This explains the generally lower amount seen in orbits 10 and 11, where lower He energies are visible because of their stronger gravitational deflection. Starting with orbit 20, we saw a transition to H at 15 eV, which was complete in orbit 23 (lower left in Table 1). In orbits 16 to 18 at 600 eV, we observed almost 100% of C+O, consistent with O calibration results (lower right in Table 1). The visibility of the interstellar neutral flow as a function of energy and longitude, together with the composition, shows that we observed interstellar He from orbit 9 through orbit 22, O simultaneously with He in orbits 14 to 18, and H after orbit 23, when the He flow vanished.

With the spin axis always in the ecliptic plane, IBEX records detailed angular distributions of the LISM flow in ecliptic latitude (Fig. 2). The interstellar flow observations started with a relatively wide distribution of He (shown for orbit 11 in Fig. 2A), with the flow pointing at about –11° into the ecliptic plane. During the passage of the main interstellar flow (orbits 14 to 18 in Fig. 2B), He showed a much narrower peak, with O about half the width of He. Their flows point at somewhat less than –4° ecliptic latitude. The H flow distribution from orbit 23 peaks about –3° in latitude and is substantially wider than the He distribution (Fig. 2C). Thus, all interstellar species flow at small negative latitude angles, consistent with the primary interstellar flow pointing at –5.3° in latitude, based on a recent analysis of several interstellar He observations (*5*).

The O peak flow appears slightly asymmetric, with a foot toward negative latitude, consistent with the average latitude of the entire distribution being 0.3° more negative than the center of the Gaussian. Also consistent with such a foot, O exhibits a tail toward higher latitude and lower longitude in viewing direction in the O sky map at 600 eV (Fig. 1D). This tantalizing finding, which warrants further investigation, points to a secondary component from charge exchange in the heliosheath, beyond the heliopause (*7*). The direction of the asymmetry is consistent with the observed deflection of the interstellar H flow toward lower latitudes compared with the primary He flow (*17*) that was interpreted as an effect of the interstellar magnetic field (*18*) and with the heliospheric asymmetry indicated by the Voyager termination shock crossings (*19*).

The width [Gaussian full width half-maximum (FWHM)] of the latitudinal He flow distribution when IBEX is looking into the flow (orbits 14 to 18) is about twice that of O. Using a convected Maxwellian with 6300 K (LISM temperature) for both species and a gravitational free-fall speed of 49.9 km s^{-1} at 1 AU, consistent with an original flow velocity of 26.3 km s^{-1} (*9*), the resulting width of the angular distributions in the moving frame of Earth is consistent with the observed He and O distributions. Because the strong radiation pressure on H mostly compensates the Sun's gravity (*20*), such a simple flow model may not be valid for H.

Simulated count rates (*21*) follow closely the observed count rates taken at the peak of the latitudinal distributions (Fig. 3). This comparison indicates that both the He and O observations by IBEX are consistent with physical He LISM flow parameters from recent studies (*5*, *9*) and with the two species having the same temperature. The interstellar H flow was seen only after He disappeared, and thus the peak in H was likely masked by the much stronger He signal. The continuing observation of H in late spring when Earth's motion pointed beyond the interstellar upwind direction and when trajectories fall into the IBEX FOV that appear deflected away from the Sun point to a strong effect of solar radiation pressure on H, as reported in previous studies (*20*).

IBEX observed the interstellar neutral gas flow distribution of three key species, H, He, and O, over a wide angular range in ecliptic longitude and latitude. A He flow distribution is presented that extends from right after Earth intercepts the gravitational focusing cone of He in December 2008 through March 2009. These combined observations provide a snapshot of the interstellar flow conditions for three species during the current extended solar minimum. Any temporal variations of these conditions are of a much longer time scale than the observation period presented here. These observations provide constraints on the interstellar flow parameters and the interaction of the interstellar flow with the heliospheric boundary. Together with future observations during different solar activity, they also constrain the ionization rates of these species and the solar radiation pressure for H.

References and Notes

1. J. L. Bertaux, J. E. Blamont, *Astron. Astrophys.* **11**, 200 (1971).
2. C. S. Weller, R. R. Meier, *Astrophys. J.* **193**, 471 (1974).
3. E. Möbius *et al.*, *Nature* **318**, 426 (1985).
4. G. Gloeckler *et al.*, *Science* **261**, 70 (1993).
5. E. Möbius *et al.*, *Astron. Astrophys.* **426**, 897 (2004).
6. M. Gruntman, *Planet. Space Sci.* **41**, 307 (1993).
7. E. Möbius *et al.*, *Space Sci. Rev.* 10.1007/s11214-009-9498-5 (2009).
8. M. Witte, M. Banaszkiewicz, H. Rosenbauer, *Space Sci. Rev.* **78**, 289 (1996).
9. M. Witte, *Astron. Astrophys.* **426**, 835 (2004).
10. P. Wurz *et al.*, *AIP Conf. Proc.* **719**, 195 (2004).
11. D. J. McComas *et al.*, *Space Sci. Rev.* 10.1007/s11214-009-9499 (2009).
12. D. J. McComas *et al.*, *Science* **326**, 959 (2009); published online 15 October 2009 (10.1126/science.1180906).
13. H. Funsten *et al.*, *Science* **326**, 964 (2009); published online 15 October 2009 (10.1126/science.1180927).
14. S. A. Fuselier *et al.*, *Science* **326**, 962 (2009); published online 15 October 2009 (10.1126/science.1180981).
15. S. A. Fuselier *et al.*, *Space Sci. Rev.* 10.1007/s11214-009-9495 (2009).
16. P. Wurz *et al.*, *J. Appl. Phys.* **103**, 10.1063/1.2842398 (2008).
17. R. Lallement *et al.*, *Science* **307**, 1447 (2005).
18. V. V. Izmodenov, D. B. Alexashov, A. V. Myasnikov, *Astron. Astrophys.* **437**, L35 (2005).
19. E. C. Stone *et al.*, *Nature* **454**, 71 (2008).
20. E. Quemerais *et al.*, *Astron. Astrophys.* **455**, 1135 (2006).
21. M. Bzowski *et al.*, *Astron. Astrophys.* **491**, 7 (2008).

22. We thank the many individuals who made this mission possible. This work is supported by NASA under contract NNG05EC85C, by the Swiss National Science Foundation, the Programme de Développement d'Expériences Scientifiques (PRODEX), the Space Research Centre of the Polish Academy of Sciences, and the Russian Federation.

24 August 2009; accepted 2 October 2009
Published online 15 October 2009;
10.1126/science.1180971
Include this information when citing this paper.

Imaging the Interaction of the Heliosphere with the Interstellar Medium from Saturn with Cassini

S. M. Krimigis,[1,2]* D. G. Mitchell,[1] E. C. Roelof,[1] K. C. Hsieh,[3] D. J. McComas[4,5]

We report an all-sky image of energetic neutral atoms (ENAs) >6 kilo–electron volts produced by energetic protons occupying the region (heliosheath) between the boundary of the extended solar atmosphere and the local interstellar medium (LISM). The map obtained by the Ion and Neutral Camera (INCA) onboard Cassini reveals a broad belt of energetic protons whose nonthermal pressure is comparable to that of the local interstellar magnetic field. The belt, centered at ~260° ecliptic longitude extending from north to south and looping back through ~80°, appears to be ordered by the local interstellar magnetic field. The shape revealed by the ENA image does not conform to current models, wherein the heliosphere resembles a cometlike figure aligned in the direction of Sun's travel through the LISM.

The quest for the dimensions and shape of the bubble of plasma called the heliosphere, created by the continuously flowing solar wind as the Sun travels through the LISM, is older than the space age (*1*). Estimates of the distance to the boundary in the general direction of the solar apex have ranged from a few astronomical units (1 AU equals the distance between Earth and Sun, 150 million km) to tens of AU (*2*–*4*). Voyager 1 and 2 (V1 and V2) crossed the termination shock (TS) at distances of 94 and 84 AU in 2004 and 2007 at +35° and –26° ecliptic latitudes, respectively [e.g., (*5*–*7*)], implying that the radial dimensions of the TS are different in time and/or location. More surprisingly, the shocked thermal plasma in the heliosheath remained supersonic because only 20% of the upstream energy density went into heating the downstream thermal plasma, while most of the rest went into heating pickup ions (PUI), including a substantial part (≥15%) going into protons >28 keV (*6*, *7*). PUI are interstellar neutrals that are ionized in the solar wind and picked up and accelerated to energies >1 keV by the flow (*8*).

The prevailing models of the shape of the heliosphere suggest a cometary-type interaction (Fig. 1) with a possible bow shock and/or heliopause, heliosheath, and TS, all foreshortened in the direction of motion of the solar system through the LISM (*3*, *9*). Energetic singly charged particles in the heliosheath will charge-exchange with interstellar neutral hydrogen and enter the heliosphere as ENAs unimpeded by the interplanetary magnetic field [e.g., (*10*, *11*)].

Launch of the ENA imager on the Cassini-Huygens mission to Saturn occurred in October 1997. The Cassini spacecraft spent nearly 7 years in interplanetary cruise with sporadic data coverage before insertion into orbit at Saturn on 1 July 2004. Because the principal objective of the Ion and Neutral Camera (INCA) instrument (*12*) (fig. S1) is to image the energetic plasma ions trapped in Saturn's magnetosphere through ENAs, it took several years to obtain a nearly full image of the heliosphere in directions away from Saturn, with a minor gap in the direction of the Sun. In October 2008, Interstellar Boundary Explorer (IBEX) was launched with ENA cameras specifically designed to map the heliospheric boundary at lower (<6 keV) energies (*13*, *14*).

Here, we present the INCA map of the sky in ~6 to 13 keV ENAs (Fig. 2A). The ENA map reveals an intensity ratio ≥ 10 between low intensities in the middle of the image and a bright, broad, latitude-dependent belt of higher intensities. The minimum reappears beyond the belt at ≥120° to about –170° at the respective edges of the image. The belt that makes a rough circle in the sky about the interstellar field direction as it extends from north to south is ~100° full width at half maximum (FWHM) at the ecliptic equator in

[1]Applied Physics Laboratory, Johns Hopkins University, Laurel, MD 20723, USA. [2]Office for Space Research and Technology, Academy of Athens, 106 79 Athens, Greece. [3]Department of Physics, University of Arizona, Tucson, AZ 85721, USA. [4]Southwest Research Institute, San Antonio, TX 78228, USA. [5]University of Texas, San Antonio, TX 78249, USA.

*To whom correspondence should be addressed. E-mail: tom.krimigis@jhuapl.edu

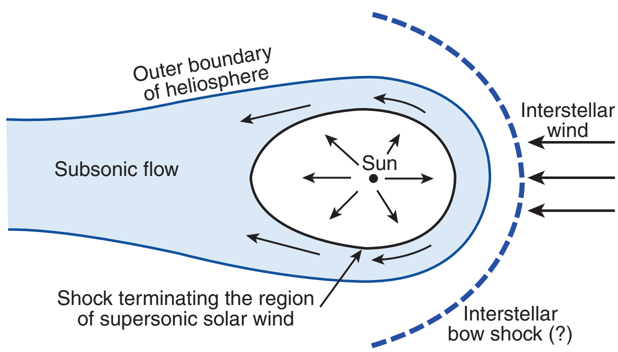

Fig. 1. Conventional concept of the heliosphere [(adapted from (*3*)]: The Sun is at the center, the region of the supersonic solar wind being asymmetric and compressed in the direction facing the interstellar wind flow (nose). Beyond the TS, the solar wind is expected to become subsonic and flow into the wake of the solar system, forming a cometlike tail.